Supporting information for

Fast ^{19}F Magic-Angle-Spinning NMR Crystallography for Structural Characterization of Fluorine-Containing Pharmaceutical Compounds

Changmiao Guo[1,2], Matthew Fritz[1,2], Jochem Struppe[4], Sebastian Wegner[5], John Stringer[6], Ivan V. Sergeyev[4], Caitlin M. Quinn[1], Angela Gronenborn[2,3*], Tatyana Polenova[1,2*]

[1]Department of Chemistry and Biochemistry, University of Delaware, Newark, Delaware 19716, United States; [2]Pittsburgh Center for HIV Protein Interactions, University of Pittsburgh School of Medicine, 1051 Biomedical Science Tower 3, 3501 Fifth Avenue, Pittsburgh, Pennsylvania 15261, United States; [3]Department of Structural Biology, University of Pittsburgh School of Medicine, 3501 Fifth Ave., Pittsburgh, PA 15261, United States; [4]Bruker Biospin Corporation, 15 Fortune Drive, Billerica, Massachusetts 01821, United States; [5]Bruker BioSpin GmbH, Rheinstetten, Germany; [6]PhoenixNMR, 510 E. 5th Streest, Loveland, CO 80537, United States

Table of contents:

MATERIALS AND METHODS

Chemicals

Natural abundance mefloquine hydrochloride was purchased from Acros Organics and used without further recrystallization. For MAS NMR experiments, sample amounts were as follows: 3 mg (1.3 mm rotor for measurements at 11.7 T), 3.7 mg (1.3 mm rotor for measurements at 14.1 T), 9.5 mg (1.6 mm rotor for measurements at 16.4 T), and 13.5 (1.9 mm rotor for measurements at 19.9 T).

MAS NMR spectroscopy

^{19}F and ^{13}C-detected experiments were performed on a 20.0 T narrow bore Bruker AVANCE III spectrometer outfitted with a 1.9 mm HX MAS probe. The Larmor frequencies were 850.4 MHz for ^{1}H, 800.1 MHz for ^{19}F and 213.8 MHz for ^{13}C. For all ^{19}F-detected experiments, the ^{1}H channel was tuned to ^{19}F. All MAS NMR spectra were acquired at a MAS frequency of 40 kHz maintained within ± 10 Hz by Bruker MAS III controller. The sample temperature was calibrated with KBr as an external temperature sensor and was maintained at 12.0±0.3 °C by a Bruker variable temperature controller. Typical 90^{o} pulse lengths were 1.5 μs for ^{1}H, 1.1 μs for ^{19}F and 3.0 μs for ^{13}C. ^{19}F chemical shifts were referenced with respect to those of trifluoroacetic acid (100 μM solution in 25 mM sodium phosphate buffer, pH 6.5) used as an external reference (0 ppm), which relates to other commonly used reference standards as: neat trifluoroacetic acid (-2.8 ppm), trichloro-fluoro-methane (73.55 ppm), Teflon (-48.45 ppm). ^{13}C chemical shifts were referenced to adamantane.

The ^{19}F-^{13}C cross-polarization was performed with a linear amplitude ramp of 70-100 % on ^{13}C and the center of ramp was Hartmann-Hahn matched at the first or second spinning sideband; the carrier frequency on ^{13}C was set to 100 ppm. For optimization of ^{19}F-^{13}C CP, ^{19}F rf fields of 15, 25, 30, 35, 45 and 55 kHz were applied, and Hartmann-Hahn matched at 1~3 times of the spinning frequency (ν_r). Zero quantum (ZQ) or double quantum (DQ) CP was matched with the ^{19}F rf field fixed while the ^{13}C rf field was systematically varied over a range of 0 kHz to 75 kHz. ^{19}F-^{13}C CPMAS spectra were acquired with 512 scans and CP contact times varied systematically from 1.0 ms to 10.0 ms; the rf fields were 15 kHz for ^{19}F and 25 kHz (DQ-CP) or 55 kHz (ZQ-CP) for ^{13}C. For 2D ^{19}F-^{13}C HETCOR experiments, the CP contact times were 1.0, 7.0 and 10.0 ms; both DQ-CP and ZQ-CP conditions were used; 38 complex points were acquired in t_2 dimension. The carrier frequencies in ^{13}C were set to 100.0 ppm. In several experiments, π-pulse ^{19}F decoupling at RF field of 208 kHz was applied during evolution in ^{13}C dimension. A recycle delay of 6.0 s was used for all experiments.

For ^{1}H-^{13}C CPMAS experiments, the ^{1}H-^{13}C cross polarization was performed with a linear ramp; the ^{1}H and ^{13}C RF fields were at 13 kHz and 28 kHz, respectively; the typical CP contact times were 0.5-1.4 ms. 2D ^{1}H-^{13}C HETCOR spectra with 0.5 ms and 1.1 ms CP contact were acquired with 448 and 384 transients, respectively; 80 complex points were collected in the indirect dimension.

2D ^{19}F-^{19}F RFDR spectra were acquired without decoupling with RFDR mixing times of 1.6 ms, 4 ms, 8 ms, 12 ms, 20 ms and 30.4 ms. The typical length of the RFDR π pulse was 8.3 μs and a XY-16 phase cycle was used during the RFDR mixing. For each ^{19}F-^{19}F spectrum, the data were collected with 120 complex points in t_2 dimension using States-TPPI phase sensitive detection; 16 transients were averaged for each FID. The 1D ^{19}F DANTE spectra were acquired with 16 scans; 22 0.1-μs DANTE pulses were applied at 8.8 ppm and 15.9 ppm for selective irradiation of $2CF_3$ and $8CF_3$ signals, respectively. The DANTE interpulse delay was set to 4 rotor cycles. The recycle delay was 5.0 s.

^{19}F-detected single pulse excitation spectra were also acquired on a 11.7 T wide bore Bruker AVANCE III spectrometer outfitted with a 1.3 mm HFX MAS probe. The Larmor frequencies were 500.13 MHz for ^{1}H and 470.59 MHz for ^{19}F. The MAS frequencies were 10, 40, and 60 kHz maintained within ±10 Hz by Bruker MAS III controller. Spinal-64[41] (10 kHz MAS) or swept-frequency two-pulse phase modulation (SW_f-TPPM)[42] heteronuclear decoupling sequences were applied with the ^{1}H RF field strengths of 90 kHz, 15 kHz, and 10 kHz for the MAS frequencies of 10 kHz, 40 kHz, and 60 kHz, respectively. ^{19}F 90° pulse length was 2.45 μs. The recycle delay was 6.0 s.

Additional 2D ^{19}F-^{19}F RFDR spectra were recorded at 14.1 T, on a Magnex narrow-bore magnet interfaced with a Bruker AVIII HD spectrometer, and outfitted with a 1.3 mm Bruker HCN MAS probe. The H channel was tuned to the ^{19}F Larmor frequency of 564.35 MHz and the typical ^{19}F 90° pulse length was 3.3 μs for. ^{19}F-^{19}F RFDR spectra were recorded for MAS frequencies of 40 kHz, 50 kHz and 60 kHz with RFDR mixing times of 3.2 ms and 8.0 ms, 16 transients were averaged and the recycle delay was 2.0 s. The pulse length for the DANTE selective excitation pulses was 0.1 μs. The interpulse delay was set to 2 rotor cycles. The DANTE-RFDR magnetization exchange curves were recorded with RFDR mixing times of 0.8, 1.6, 3.2, 4.0, 5.6, 8.0, 12.0, 16.0, 21.6, 26.4, and 30.4 ms; $(XY8)^1_4$ phase cycle[43] was applied during the RFDR mixing.

Supplemental ^{19}F-^{13}C CPMAS and HETCOR NMR spectra were acquired on a 16.4 T Bruker spectrometer equipped with a PhoenixNMR 1.6 mm HFX MAS probe at a MAS frequency of 40 kHz. The Larmor frequencies were 700.1 MHz for ^{1}H, 658.8 MHz for ^{19}F and 176.0 MHz for ^{13}C. The typical 90° pulse lengths were 2.5 μs for ^{1}H, 2.0 μs for ^{19}F, and 1.97 μs for ^{13}C. The ^{19}F-^{13}C CP contact time was 7.0 ms. ^{1}H and ^{19}F decoupling was applied simultaneously during the t_2 evolution in the ^{13}C dimension. ^{1}H decoupling used low-power XiX[35] with an rf field of 12.5 kHz. For ^{19}F decoupling, a π-pulse with the rf field of 125 kHz was applied every rotor period. A spin echo ^{1}H π-pulse was applied in the center of the t_1 evolution in the ^{19}F dimension to refocus the ^{1}H offset and heteronuclear coupling. The recycle delay was 3 s.

All spectra were processed in TopSpin 4.0 and analyzed with Sparky[44] and Mnova.

Numerical simulations

The DANTE-RFDR magnetization exchange curves were simulated using SIMPSON[45] (version 3.1.0). In the multi-spin simulation, the magnetization exchange was followed starting from the non-selectively irradiated spin and the evolution of the spin to which the magnetization is transferred was performed from I_{2x} to $-I_{1z}$. The experimental decay curves of the signals that are selectively excited by the DANTE pulse are scaled to 1 and the experimental buildup curves of the nonselective signals are scaled to 0. The simulated DANTE-RFDR exchange curves were rescaled to match the experimental intensities. The example simulation script is present in the Supporting Information.

DFT calculations

^{19}F and ^{13}C magnetic shielding tensor calculations were carried out in Gaussian 09 (Revision D.01)[46]. Molecular clusters of mefloquine comprising 8 molecules were generated from the crystal structures by Pymol[47]. All-atom geometry optimizations were performed using a M06 functional with the cc-pVTZ basis set and geometry-optimized models were used for magnetic shielding tensor calculations at the same level of theory. The chemical shifts were referenced by converting absolute magnetic shieldings σ into frequencies, using the relation $\delta_i = \sigma_{ref} - \sigma_i$ with the value of σ_{ref} determined by linear regression between calculated and experimental shifts[48].

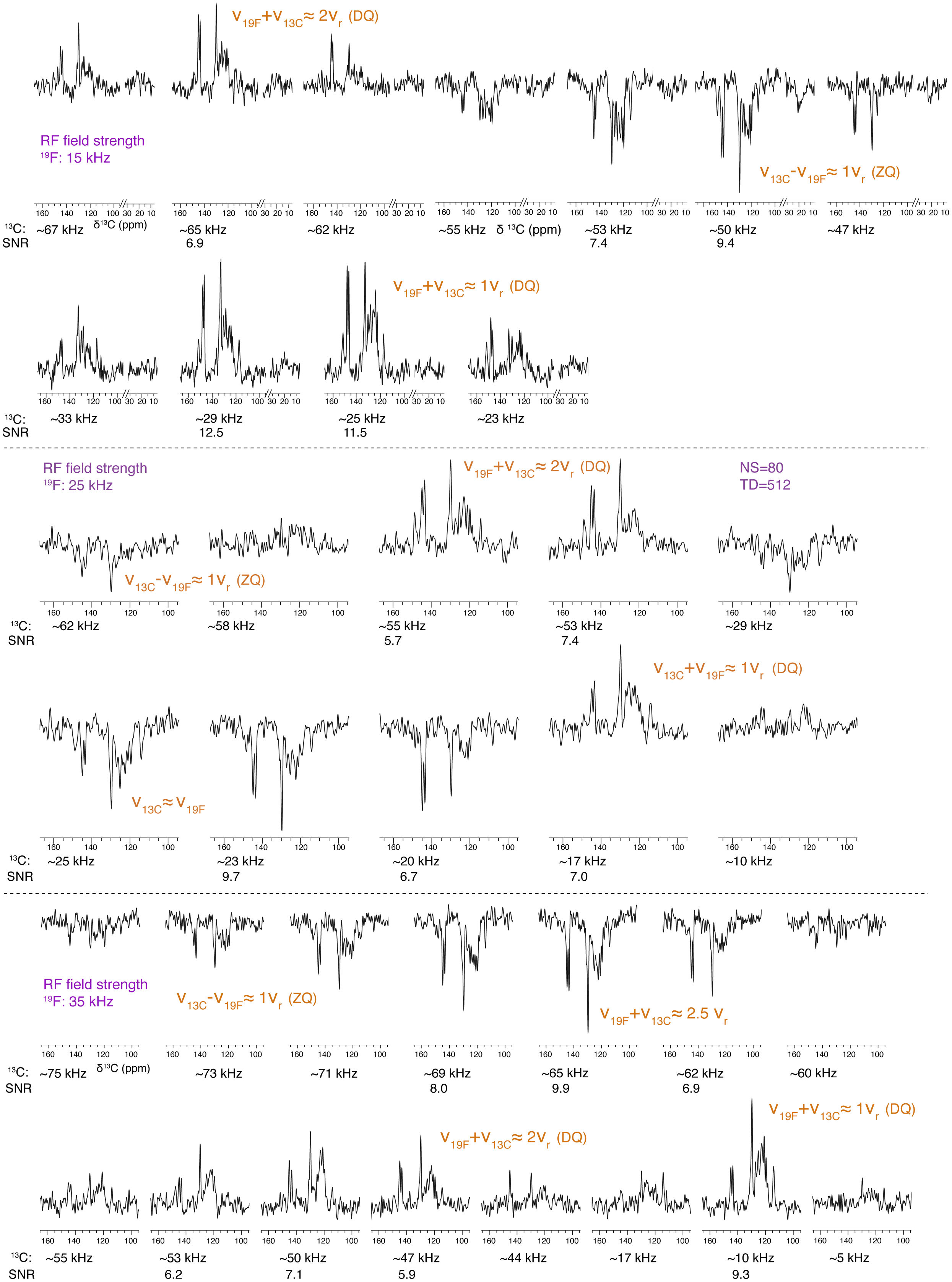

$\nu_{19F}+\nu_{13C} \approx 2\nu_r$ (DQ)
RF field strength
^{19}F: 15 kHz
$\nu_{13C}-\nu_{19F} \approx 1\nu_r$ (ZQ)
δ^{13}C (ppm)
^{13}C: ~67 kHz ~65 kHz ~62 kHz ~55 kHz ~53 kHz ~50 kHz ~47 kHz
SNR 6.9 7.4 9.4
$\nu_{19F}+\nu_{13C} \approx 1\nu_r$ (DQ)
^{13}C: ~33 kHz ~29 kHz ~25 kHz ~23 kHz
SNR 12.5 11.5
RF field strength
^{19}F: 25 kHz
$\nu_{19F}+\nu_{13C} \approx 2\nu_r$ (DQ)
NS=80
TD=512
$\nu_{13C}-\nu_{19F} \approx 1\nu_r$ (ZQ)
^{13}C: ~62 kHz ~58 kHz ~55 kHz ~53 kHz ~29 kHz
SNR 5.7 7.4
$\nu_{13C}+\nu_{19F} \approx 1\nu_r$ (DQ)
$\nu_{13C} \approx \nu_{19F}$
^{13}C: ~25 kHz ~23 kHz ~20 kHz ~17 kHz ~10 kHz
SNR 9.7 6.7 7.0
RF field strength
^{19}F: 35 kHz
$\nu_{13C}-\nu_{19F} \approx 1\nu_r$ (ZQ)
$\nu_{19F}+\nu_{13C} \approx 2.5\ \nu_r$
^{13}C: ~75 kHz ~73 kHz ~71 kHz ~69 kHz ~65 kHz ~62 kHz ~60 kHz
SNR 8.0 9.9 6.9
$\nu_{19F}+\nu_{13C} \approx 1\nu_r$ (DQ)
$\nu_{19F}+\nu_{13C} \approx 2\nu_r$ (DQ)
^{13}C: ~55 kHz ~53 kHz ~50 kHz ~47 kHz ~44 kHz ~17 kHz ~10 kHz ~5 kHz
SNR 6.2 7.1 5.9 9.3

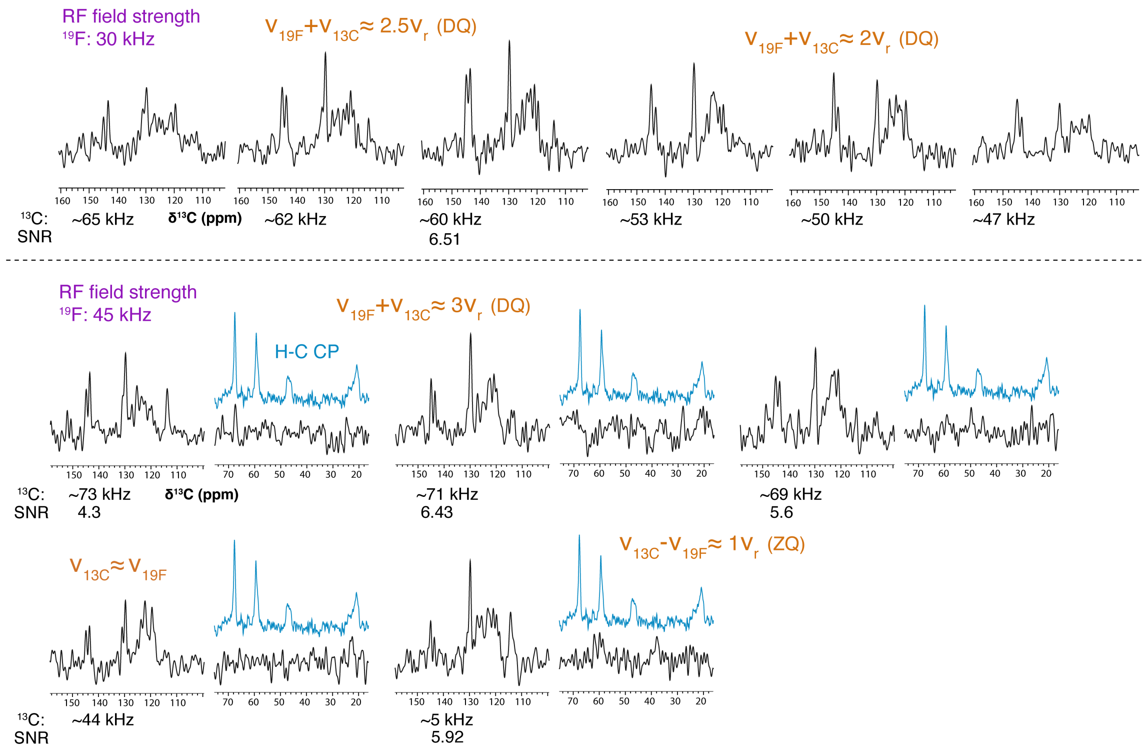

Figure S1. 1D ^{19}F-^{13}C CPMAS spectra of mefloquine acquired at various Hartmann-Hahn matching conditions (gray). The optimizations of the DQ and ZQ CP conditions were performed with the ^{19}F RF field strength fixed and the ^{13}C RF field systematically varied over the range of 0 kHz to 75 kHz. The CP contact time was 6 ms. Spectra are presented only for the matching conditions resulting in ^{19}F-^{13}C signals. The SNR and ^{13}C RF fields are shown under each spectrum. All the 1D ^{19}F-^{13}C spectra were acquired at 20.0 T with 80 scans. The aliphatic region of the corresponding ^{1}H-^{13}C CPMAS spectrum (light blue) is shown above each ^{19}F-^{13}C data set acquired with the ^{19}F rf field strength set at 45 kHz, to indicate the peak positions of the aliphatic carbons. The ^{1}H-^{13}C spectrum was acquired with 16 scans. The MAS frequency in all experiments was 40 kHz.

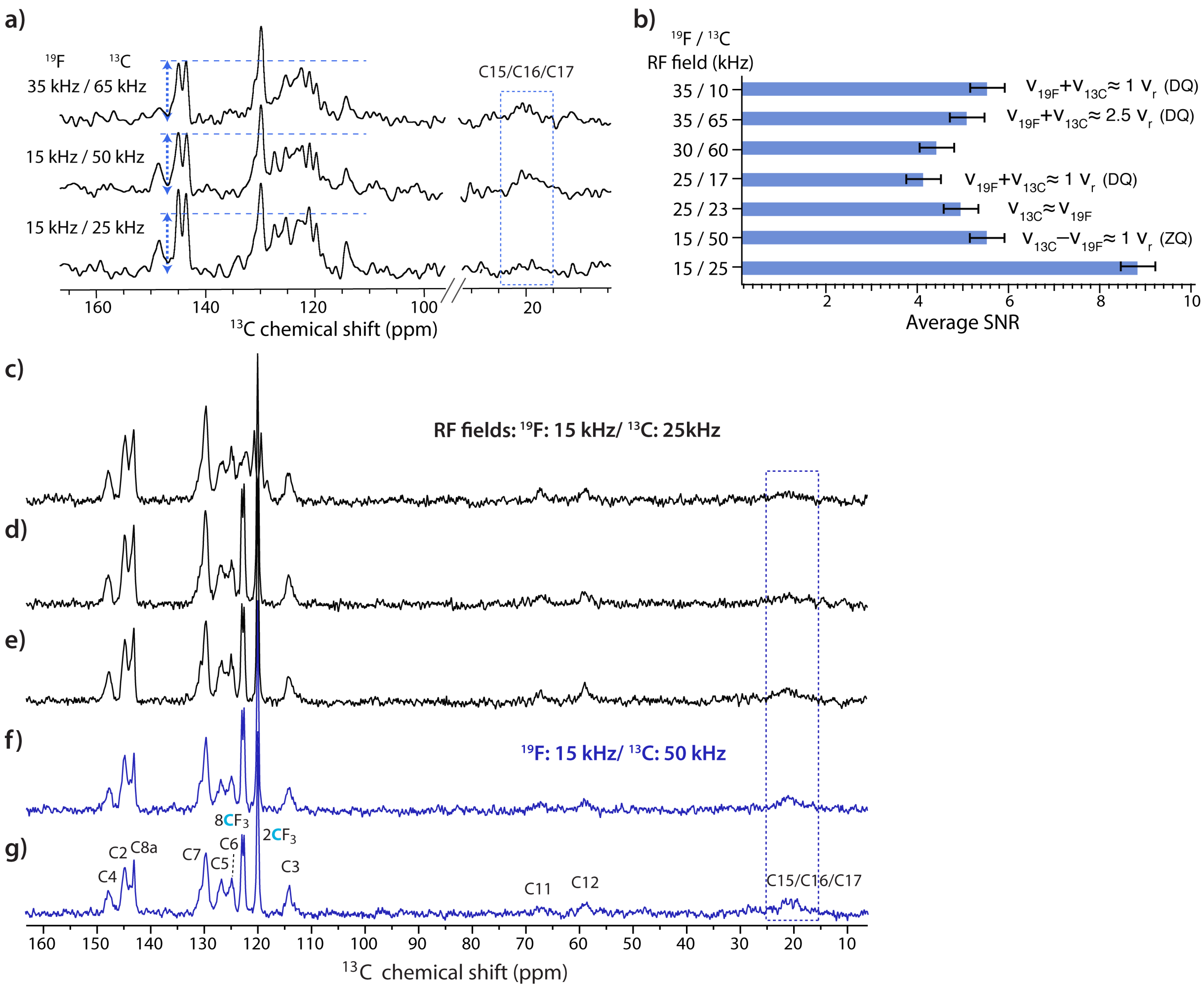

Figure S2. a) ^{19}F-^{13}C CPMAS spectra acquired at the three most efficient Hartmann-Hahn matching conditions as indicated next to each trace. The MAS frequency was 40 kHz; 80 scans were added for each spectrum. (b) Comparison of the average SNR for the aromatic signals at the different Hartmann-Hahn matching conditions. c)-g) ^{19}F-^{13}C CPMAS spectra of mefloquine acquired with the CP contact time of 7 ms without decoupling (c) and with ^{19}F decoupling (d-g). The CP contact times were set to 7 ms (d, f) and 10 ms (e, g). The ^{19}F rf field strength was 15 kHz; the ^{13}C RF field was set to 25 kHz (c, d, e) or 50 kHz (f, g). The spectra were acquired with 512 scans.

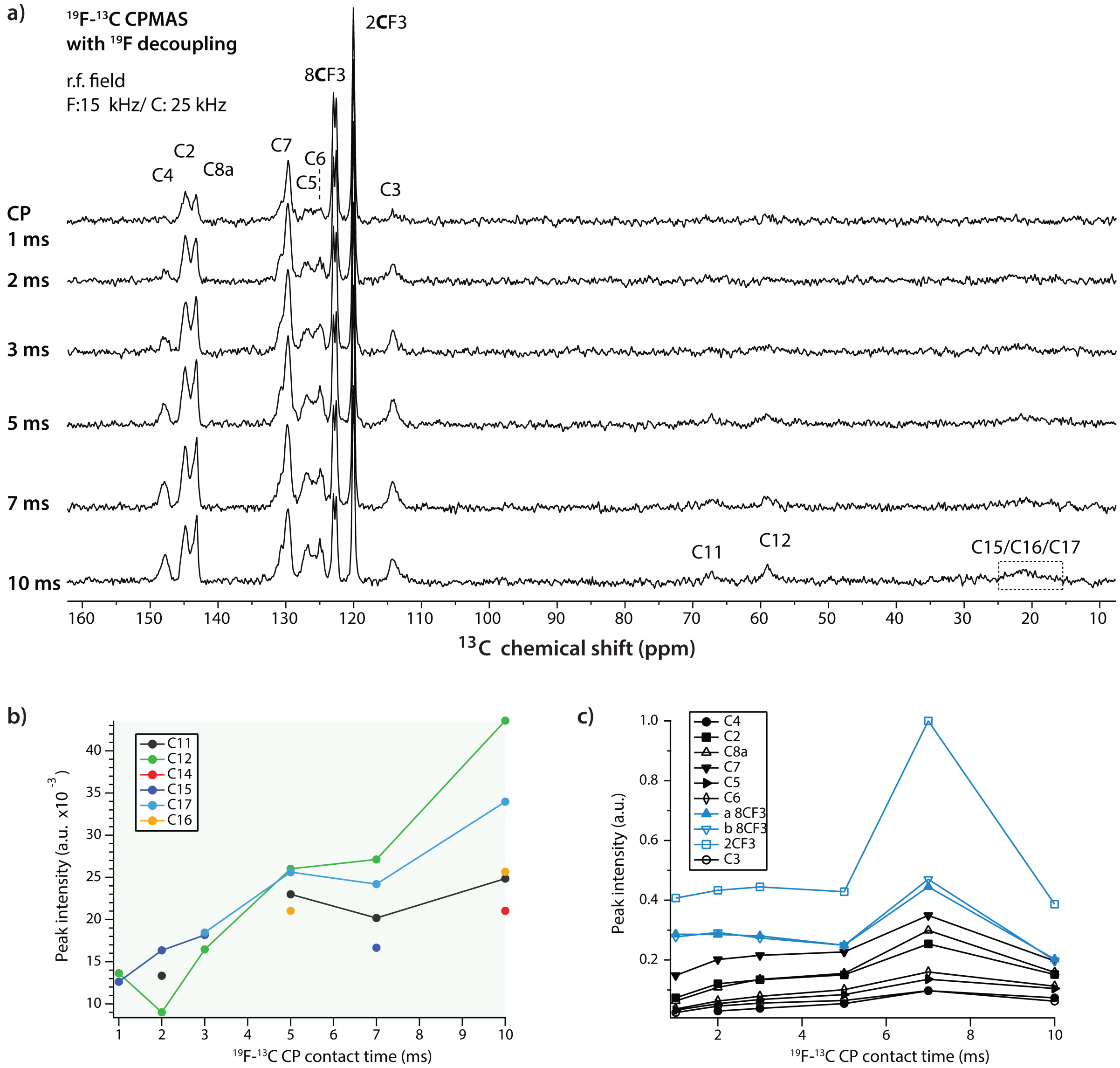

Figure S3. a) ^{19}F-^{13}C CPMAS spectra acquired with different contact times. The ^{19}F and ^{13}C rf fields were set at 15 kHz and 25 kHz, respectively. All spectra were acquired at 20.0 T; 512 transients were added for each data set. The MAS frequency was 40 kHz. b),c) ^{19}F-^{13}C CP buildup profiles for aliphatic and aromatic carbons, respectively.

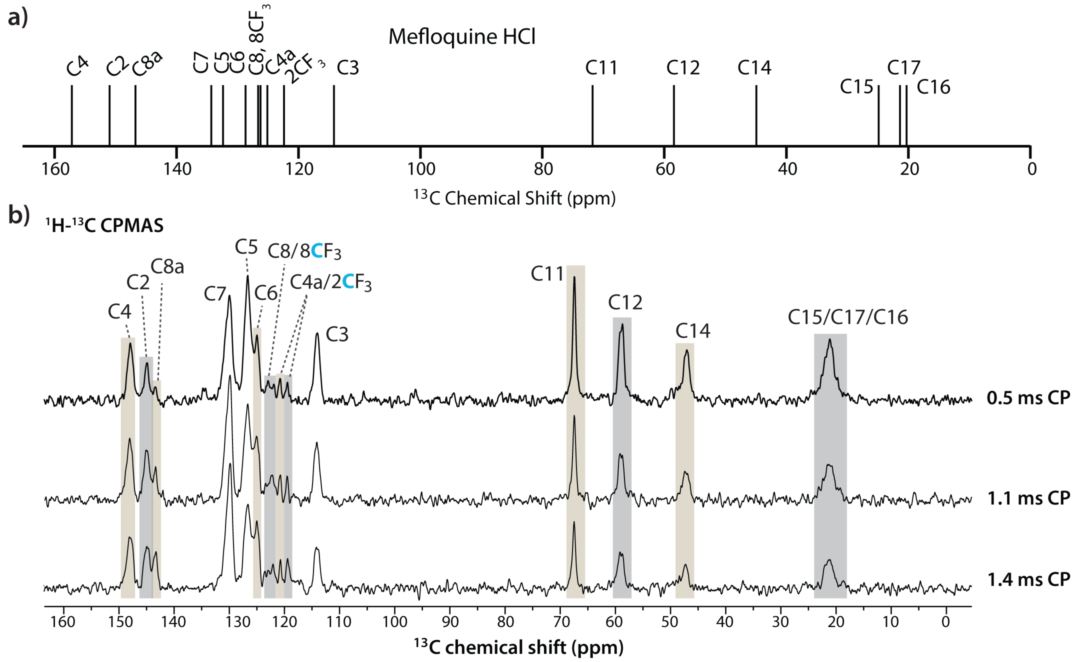

Figure S4. a) Isotropic ^{13}C chemical shifts of mefloquine obtained by DFT calculations. b) ^{1}H-^{13}C CPMAS spectra of mefloquine; the CP contact times are indicated next to each trace. The spectra were acquired at 20.0 T; 512 transients were added for each data set. The MAS frequency is 40 kHz. The ^{1}H and ^{13}C rf field strengths were 15 kHz and 25 kHz, respectively. The assignments for ^{13}C resonances are shown.

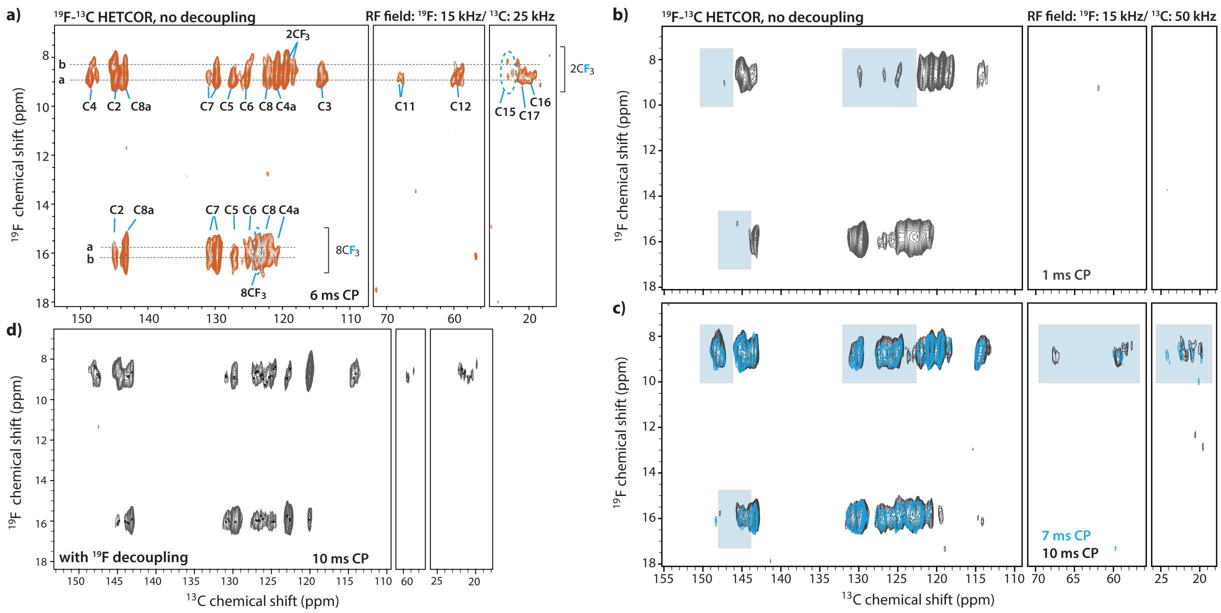

Figure S5. 2D ^{19}F-^{13}C HETCOR spectra of mefloquine. No decoupling was applied during the acquisition of spectra shown in a)-c). ^{19}F decoupling was used for the spectrum shown in (d). The contact times and the rf powers are shown next to the spectra. All spectra were acquired at 20.0 T; the MAS frequency was 40 kHz.

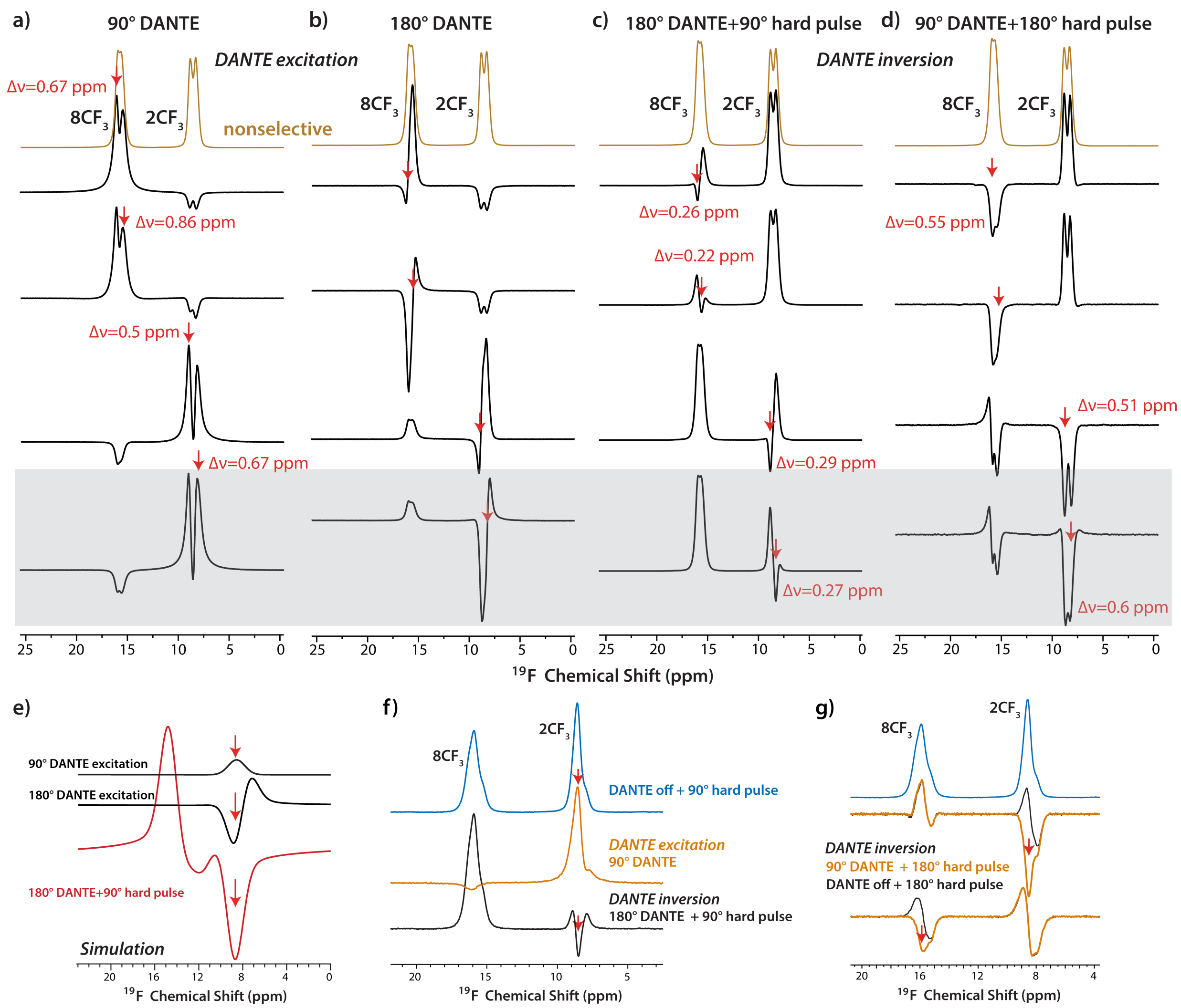

Figure S6. a)-d) ^{19}F MAS spectra of mefloquine. Brown traces: single-pulse excitation spectra. Black traces: spectra with DANTE selective pulses applied at indicated frequencies for the following pulse schemes: a) 90° DANTE excitation, b) 180° DANTE inversion, c) 180° DANTE inversion followed by a 90° non-selective pulse, and d) 90° DANTE excitation followed by a 180° non-selective pulse. The spectra were acquired with 16 scans and DANTE interpulse delays of 4 rotor cycles (4 τ_r). The arrows indicate the positions at which the DANTE pulses were applied. The widths of selected peaks are shown. e) Simulated ^{19}F DANTE excitation and inversion spectra. The DANTE pulses were applied on the $2CF_3$ resonances. f) Comparison of ^{19}F spectra acquired with 90° DANTE excitation (orange) and 180° DANTE inversion followed by a 90° non-selective pulse (black). The control nonselective single-pulse excitation spectrum is shown in blue. g) Comparison of ^{19}F spectra acquired with 90° DANTE excitation followed by a 180° non-selective pulse (orange) and the control spectra acquired with 180° non-selective pulse (black). The control nonselective single-pulse excitation spectrum is shown in blue. The spectra in f) and g) were acquired with 192 scans; the DANTE delay was $2\tau_r$. The spectra were acquired at 20.0 T (a-d) and 14.1 T (f-g); the MAS frequency was 40 kHz.

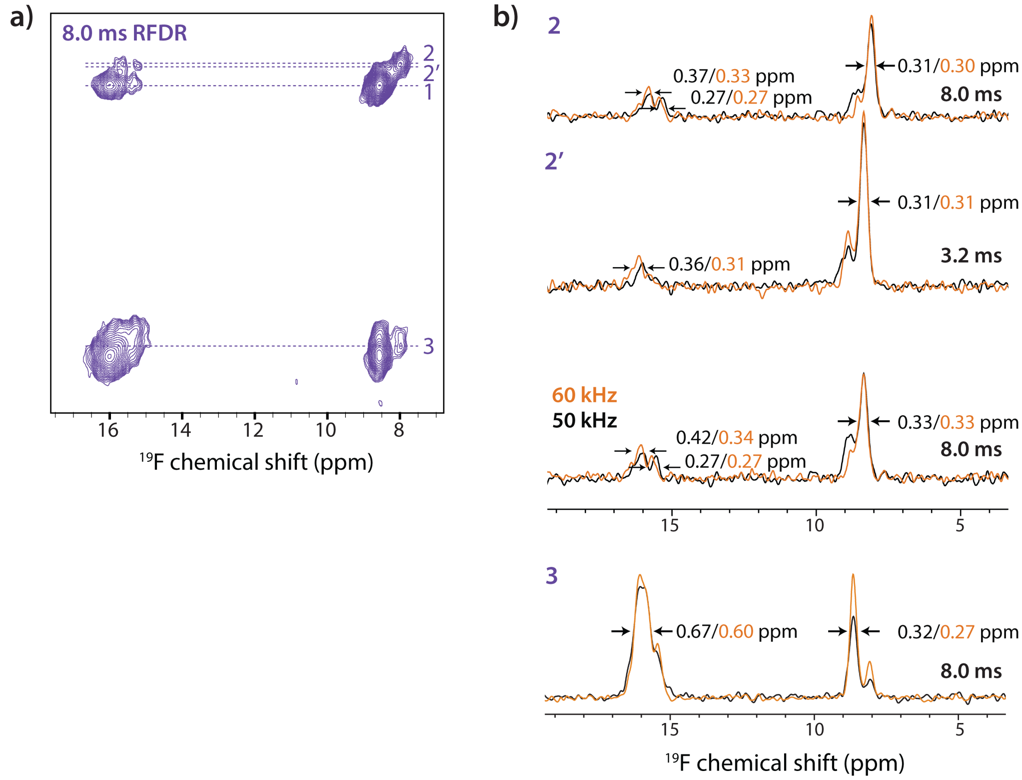

Figure S7. a) 2D ^{19}F-^{19}F RFDR spectra acquired at the MAS frequency of 50 kHz. The RFDR mixing was 8.0 ms. b) 1D slices of the 2D ^{19}F-^{19}F spectra extracted at positions indicated in a). The peak widths are indicated for the spectra acquired with the MAS frequencies of 50 kHz and 60 kHz in black and orange, respectively.

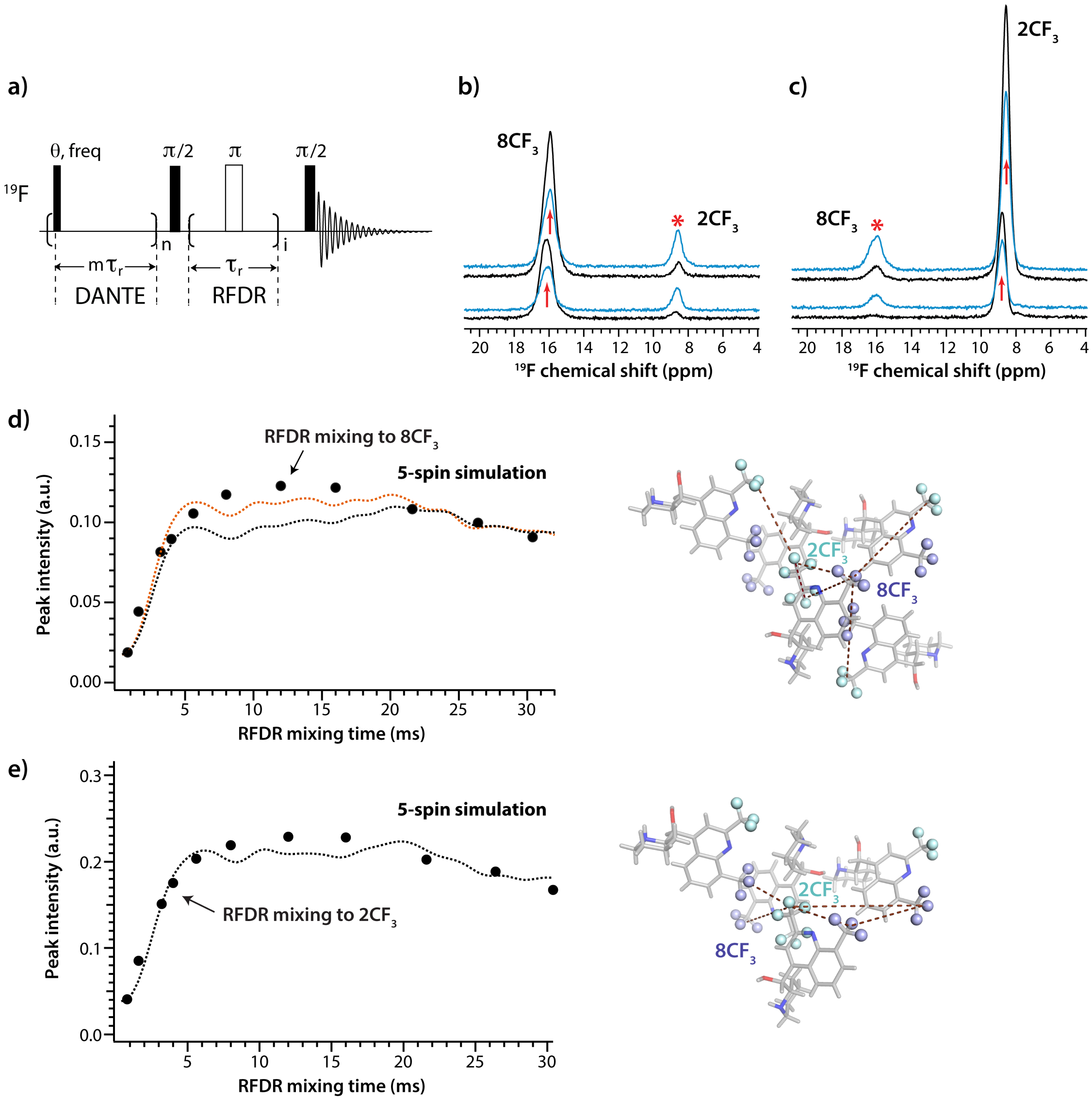

Figure S8. a) Pulse sequence for the 1D RFDR experiment with ^{19}F DANTE-excitation. b),c) 1D ^{19}F-^{19}F DANTE-RFDR spectra with DANTE 90° selective excitation applied to the ^{19}F resonances of $2CF_3$ (b) and $8CF_3$ (c), respectively. Spectra acquired with RFDR mixing times of 1.6 ms and 8.0 ms are shown in black and blue, respectively. The position of the DANTE excitation is shown with arrows and the resonances to which the magnetization was transferred by asterisks. d),e) Left: Experimental and simulated ^{19}F-^{19}F DANTE-RFDR magnetization exchange curves for the $8CF_3$ (d) and $2CF_3$ (e) resonances. The experimental data points are shown as black circles, the simulated curves, as dashed lines. In d), the $2CF_3$ spins were excited by DANTE pulses and magnetization was transferred to the $8CF_3$ spins during RFDR mixing period. In e), DANTE excitation was applied to the $8CF_3$ resonances and magnetization was transferred to the $2CF_3$ groups. Errors in the data points as defined by the standard deviation of the noise in a region of over 10 ppm are smaller than the size of the circles. The RMSDs of the simulated DANTE-RFDR magnetization exchange curves (dashed lines) are 0.008 (orange, the $2CF_3$ – $2CF_3$ distance is 7.2 Å) and 0.014 (black, the $2CF_3$ – $2CF_3$ distance is 7.4 Å) for $8CF_3$ (d) and 0.014 for $2CF_3$ (e). Right: Sets of interfluorine distances used in the 5-spin simulations, see also Table S4.

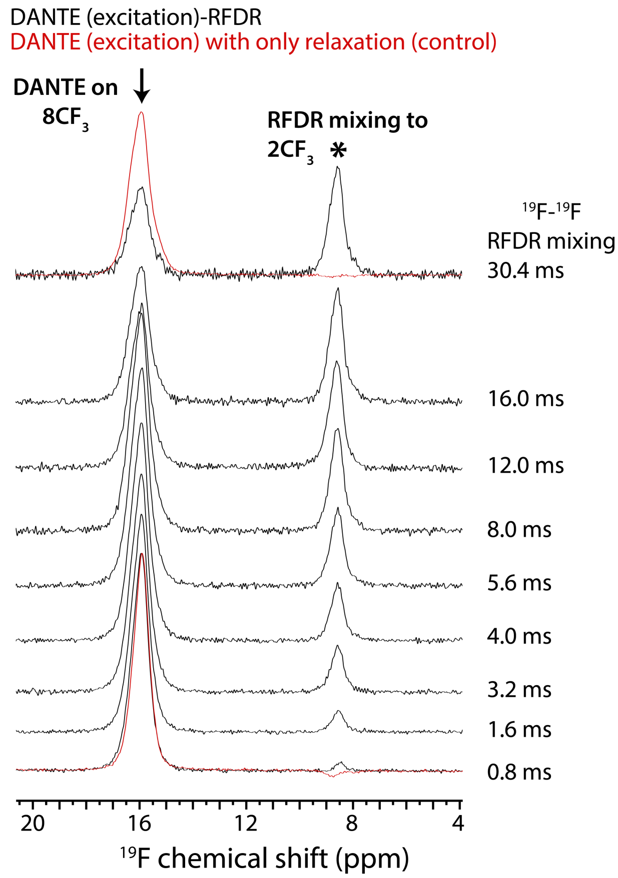

Figure S9. 1D ^{19}F DANTE-RFDR spectra of mefloquine with various RFDR mixing times (black). Following the selective excitation of $8CF_3$ signals by DANTE pulses, the magnetization was transferred to $2CF_3$ during ^{19}F-^{19}F RFDR mixing. The control experiments where the RFDR mixing is absent are shown in red. The spectra were acquired at 14.1 T. The MAS frequency was 40 kHz.

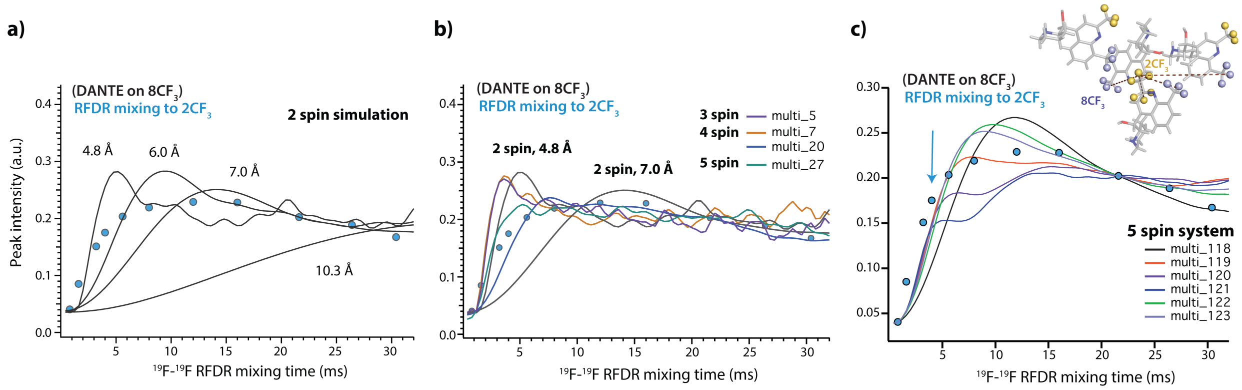

b)

	Distances (Å) 2CF$_3$-8CF$_3$				8CF$_3$-8CF$_3$
5	4.8	8.4			5
7	4.8	8.4	10.3		5
20	7	8.4	10.3		6
27	7	8.4	10.3	**5.2**	6

c)

	Distances (Å) 2CF$_3$-8CF$_3$			2CF$_3$-2CF$_3$
118	7	10.3	8.4	
119	7	10.3	8.4	**6.5**
120	7	10.3	8.4	**6**
121	7	10.3	8.4	**5.6**
122	7	10.3	8.4	**7.4**
123	7	10.3	8.4	**7**

Figure S10. a)-c) Experimental and simulated ^{19}F DANTE-RFDR magnetization exchange profiles of the 2CF$_3$ moiety. The experimental data are shown as cyan circles, and the simulated curves as solid lines. The simulations with two-spin systems (a) and multispin simulations with 3-spin, 4spin and 5-spin systems (b) were performed using the ^{19}F-^{19}F distances from the crystal structure. Simulations with different ^{19}F-^{19}F distances are color coded and the corresponding distances used for each simulation are indicated in the plots or listed in the tables. The interfluorine distance between spin 1 (on which DANTE selective excitation was applied) and spin 2 (to which magnetization was transferred during RFDR mixing period) is shown in a dashed box, for each set of the simulations. The multispin models used in the simulations are illustrated in the top right of c).

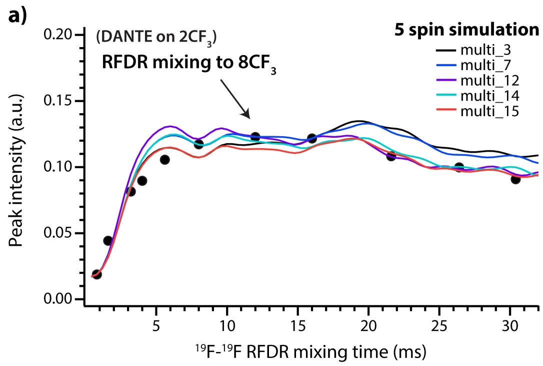

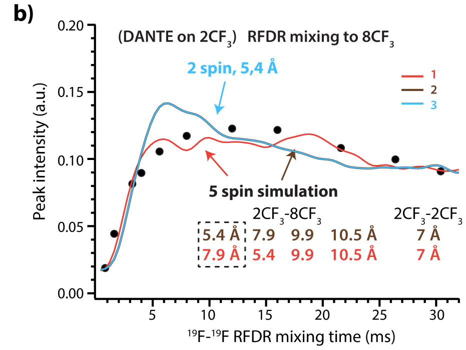

	Distances (Å) 2CF$_3$-8CF$_3$				2CF$_3$-2CF$_3$	RMSD
3	7.9	10.5	9.5	5.4	7	0.012
7	7.9	10.5	9.5	**5.5**	7	0.012
12	7.9	10.5	9.5	5.4	**6.7**	0.012
14	7.9	10.5	9.5	**5.5**	**6.85**	0.009
15	7.9	10.5	9.5	5.4	**6.85**	0.008

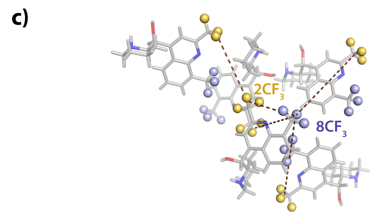

Figure S11. a) Experimental and simulated ^{19}F DANTE-RFDR magnetization exchange curves of the 8CF$_3$ moiety. The experimental data are shown as black circles. The multispin model used in the simulations is illustrated at the top. Simulations with different ^{19}F-^{19}F distance sets are color coded and the corresponding distances are listed in the tables. The interfluorine distance between spin 1 (on which DANTE selective excitation was applied) and spin 2 (to which magnetization was transferred during RFDR mixing period) is shown in the dashed box, for each set of the simulations. b) Comparison of the 2-spin (cyan trace) and 5-spin (red and brown traces) simulations demonstrating the multispin effects and the dominant influence of the shortest distance on the initial magnetization buildup. c) Multispin models used for the 5-spin simulations of 8CF$_3$ moiety.

Table S1. Signal-to-noise ratios (SNR) for the most efficient ^{19}F-^{13}C CP conditions identified for mefloquine. The MAS frequency was 40 kHz.

Hartmann-Hann matching conditions	Magnetization transfer	^{19}F rf field	^{13}C rf field	SNR
$\nu_{19F} + \nu_{13C} \approx 1\ \nu_r$	double quantum (DQ)	15	25	8.8
$\nu_{13C} - \nu_{19F} \approx 1\ \nu_r$	zero quantum (ZQ)	15	50	5.5
$\nu_{13C} \approx \nu_{19F}$	zero quantum (ZQ)	25	23	4.9
$\nu_{19F} + \nu_{13C} \approx 1\ \nu_r$	DQ	25	17	4.1
–	–	30	60	4.4
$\nu_{19F} + \nu_{13C} \approx 2.5\ \nu_r$	DQ	35	65	5.1
$\nu_{19F} + \nu_{13C} \approx 1\ \nu_r$	DQ	35	10	5.5

Table S2. MAS NMR Experimental and DFT Calculated ^{13}C Isotropic Chemical Shifts and Interatomic Distances in Mefloquine

Carbon atom	$\delta^{13}C$ (ppm) MAS NMR		$\delta^{13}C$ (ppm) DFT	Distance to ^{19}F (Å)	
	a	b		2C**F**3	8C**F**3
C4	147.5	148	157.2	4.5*	5.2
C2	144.3	145	150.9	2.3	4.1
C8a	143.6	143.2	146.7	4.1	3
C7	129.7		134.3	6.3	3.4
C5	126.8		132.4	6.2	4.9
C6	125.2	124.7	128.7	6.8	4.6
8**C**F3	123.0	122.6	126.2	5	1.3
C8	122.2#		126.6	5	2.4
C4a	120.8#		125.1	4.9	4.3
2**C**F3	120.1		122.4	1.3	4.7
C3	114.3	114.1	114.2	3.4	5.2
C11	67.7		71.7	5.8	6.7
C12	59.3	58.8	58.4	6.3	7
C14	47		44.9	8.5	9
C15	23.1, 22.4	(22.3-23.6)	24.8	8.1	9.1
C17	21.7, 21.4	(21.3-22.0)	21.4	5.7	7
C16	21.0, 20.1	(19.8-20.9)	20.3	6.8	7.7

*Resonances were assigned on the basis of ^{19}F-^{13}C CPMAS, ^{1}H-^{13}C CPMAS and ^{19}F-^{13}C HETCOR spectra. Correlations detected in 2D FC-HETCOR with the 7.0 ms CP contact time are highlighted in green and those only detected with the 1ms CP contact in light green.

Table S3. Intramolecular and intermolecular ^{19}F-^{19}F distances (Å) in the mefloquine crystal structure*

Residue	**a** $2CF_3$	**a** $8CF_3$	**b** $2CF_3$	**b** $8CF_3$	**c** $2CF_3$	**c** $8CF_3$
a $2CF_3$	4.5	**5.4**				
a $8CF_3$	**7.9/8.0**	12.9				
b $2CF_3$	7.4/7.4/10.6/10.6	10.6/10.6/11.3/11.3	17.8	**5.4**		
b $8CF_3$	**4.5**/4.7/6.0/6.0	5.4/5.5/10.0/10.0	13.2/13.2	9.7		
c $2CF_3$	12.8/15.5/–/–	10.7/10.9/16.7/–	11.8/14.2/–/–	11.9/15.1/–/–	**10.5**	**5.4**
c $8CF_3$	**9.9/10.5**/17.3/–	**6.9/7.0**/17.7/–	10.6/15.7/–/–	7.8/17.7/–/–	8.3/14.9/–/–	13.7

*The distances between CF_3 groups were measured using spherical pseudoatoms at the geometry center of the three fluorine atoms in each CF_3 group.

The intramolecular and intermolecular distances are marked in light blue and orange, respectively. Intermolecular distances longer than 18 Å are not included.

Table S4. Sets of Interfluorine Distances for the 5-spin Simulations and in the X-ray Crystal Structure

Type of Interfluorine Distances	Simulation	X-ray
2C**F**$_3$ – 8C**F**$_3$	5.5 Å 8.0 Å 9.9 Å 10.5 Å	5.5 Å 8.0 Å 9.9 Å 10.5 Å
2C**F**$_3$ – 2C**F**$_3$ (Simulation for 8CF$_3$ resonance)	7.4 Å / 7.2 Å 10.6 Å	7.4 Å
8C**F**$_3$ – 8C**F**$_3$ (Simulation for 2CF$_3$ resonance)	7.0 Å	7.0 Å

Example simulation script

SIMPSON script for multispin simulation of DANTE(excitation)-RFDR magnetization exchange curves using the XY814 phase cycling scheme. The simulated curves need to be rescaled to match the intensities of experimental measurements. The simulation script for 2CF_3 groups with 5-spin systems is shown as an example.

```
spinsys {
  channels 19F
  nuclei 19F 19F 19F 19F 19F
  shift 1 3.65p 40p 0 0 0 0
  shift 2 -3.65p 40p 0 0 0 0
  shift 3 3.65p 40p 0 0 0 0
  shift 4 3.65p 40p 0 0 0 0
  shift 5 3.65p 40p 0 0 0 0
  dipole 1 2 -207.873 0 60 0
  dipole 3 2 -91.9389 0 60 0
  dipole 4 2 -109.689 0 60 0
  dipole 5 2 -639.704 0 60 0
  dipole 1 3 -310.294 0 60 0
}

par {
  proton_frequency 599.8e6
  spin_rate       40000
  sw              spin_rate/32
  np              80
  crystal_file    zcw615
  gamma_angles    13
  start_operator  I2x
  detect_operator -I1z

  verbose         1101
  variable FRF   73000
  variable FRF2  73000
  variable tr 1.0e6/spin_rate
}

proc pulseq {} {
  global par
  maxdt 2

  set taur [expr 1.0e6/$par(spin_rate)]
  set F180 [expr 0.5e6/$par(FRF)]
  set tau1 [expr $taur-$F180]
  set tau2 [expr $tau1/2.0]
#set tau1 [expr $taur/2]
#set tau2 [expr $tau1/2]

  reset
# ----- RFDR (XY814) ------------------

  delay $tau2

   pulse $F180 $par(FRF2) 0
  delay $tau1
   pulse $F180 $par(FRF2) 90
  delay $tau1
   pulse $F180 $par(FRF2) 0
  delay $tau1
   pulse $F180 $par(FRF2) 90
  delay $tau1
```

```
   pulse $F180 $par(FRF2) 90
  delay $tau1
   pulse $F180 $par(FRF2) 0
  delay $tau1
   pulse $F180 $par(FRF2) 90
  delay $tau1
   pulse $F180 $par(FRF2) 0
  delay $tau1
   pulse $F180 $par(FRF2) 90
  delay $tau1
   pulse $F180 $par(FRF2) 180
  delay $tau1
   pulse $F180 $par(FRF2) 90
  delay $tau1
   pulse $F180 $par(FRF2) 180
  delay $tau1
   pulse $F180 $par(FRF2) 180
  delay $tau1
   pulse $F180 $par(FRF2) 90
  delay $tau1
   pulse $F180 $par(FRF2) 180
  delay $tau1
   pulse $F180 $par(FRF2) 90
  delay $tau1
   pulse $F180 $par(FRF2) 180
  delay $tau1
   pulse $F180 $par(FRF2) 270
  delay $tau1
   pulse $F180 $par(FRF2) 180
  delay $tau1
   pulse $F180 $par(FRF2) 270
  delay $tau1
   pulse $F180 $par(FRF2) 270
  delay $tau1
   pulse $F180 $par(FRF2) 180
  delay $tau1
   pulse $F180 $par(FRF2) 270
  delay $tau1
   pulse $F180 $par(FRF2) 180
  delay $tau1
   pulse $F180 $par(FRF2) 270
  delay $tau1
   pulse $F180 $par(FRF2) 0
  delay $tau1
   pulse $F180 $par(FRF2) 270
  delay $tau1
   pulse $F180 $par(FRF2) 0
  delay $tau1
   pulse $F180 $par(FRF2) 0
  delay $tau1
   pulse $F180 $par(FRF2) 270
  delay $tau1
   pulse $F180 $par(FRF2) 0
  delay $tau1
   pulse $F180 $par(FRF2) 270
  delay $tau2
# ----- RFDR  (XY814)------------------

  store 1
#set i to 1 and accumulate
  reset
  for {set i 1} {$i <= 1} {incr i} {
    prop 1
  }
```

```
  store 10
  store 100

  reset
  acq

  for {set i 2} {$i <= $par(np)} {incr i} {
    reset
    prop 100
    acq
    reset
    prop 100
    prop 10
    store 100
  }
}

proc main {} {
  global par
  set File [open "$par(name).res" w]
  set f [fsimpson]
  faddlb $f -0 0
 fsave $f $par(name).fid
  for {set i 1} {$i <= $par(np)} {incr i} {
 #   set duration [expr $i*16*$par(tr)]
    set Sr [findex $f $i -re]
    set Si [findex $f $i -im]
    puts $File "[expr sqrt($Sr*$Sr+$Si*$Si)/2.0]"
  }
  funload $f
  close $File
}
```